AI/ML Applications in Astronomy and Astrophysics, 6-10 Jan, 2025, IUCAA

ANN-Based Global 21-cm Signal Extraction with Chromatic Ionospheric Effects

Anshuman Tripathi
Department of Astronomy, Astrophysics and Space Engineering
Indian Institute of Technology, Indore (IITI)

Collaborators: Abhirup Datta (IITI), Madhurima Choudhury (Brown University, USA), Suman Majumdar (IITI), Gursharanjit Kaur (PAS, IITI)

Observation of 21-cm Signal

$$\delta T_b(\nu) = \frac{T_s - T_\gamma}{1+z}(1 - \exp^{-\tau_{\nu_0}})$$

$$\delta T_b \approx 27(1-x_i)\left(\frac{\Omega_{b,0}h^2}{0.023}\right)\left(\frac{0.15}{\Omega_{m,0}h^2}\frac{1+z}{10}\right)^{1/2}\left(1-\frac{T_\gamma}{T_s}\right)$$

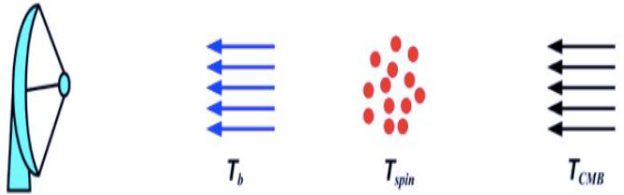

Field 1959; Pritchard & Loeb 2012

Observing type: Single radiometer

Signal: Global 21-cm Signal

Experiments: EDGES, SARAS, BigHorns, LEDA, REACH, MIST, SEAMS, PRATUSH

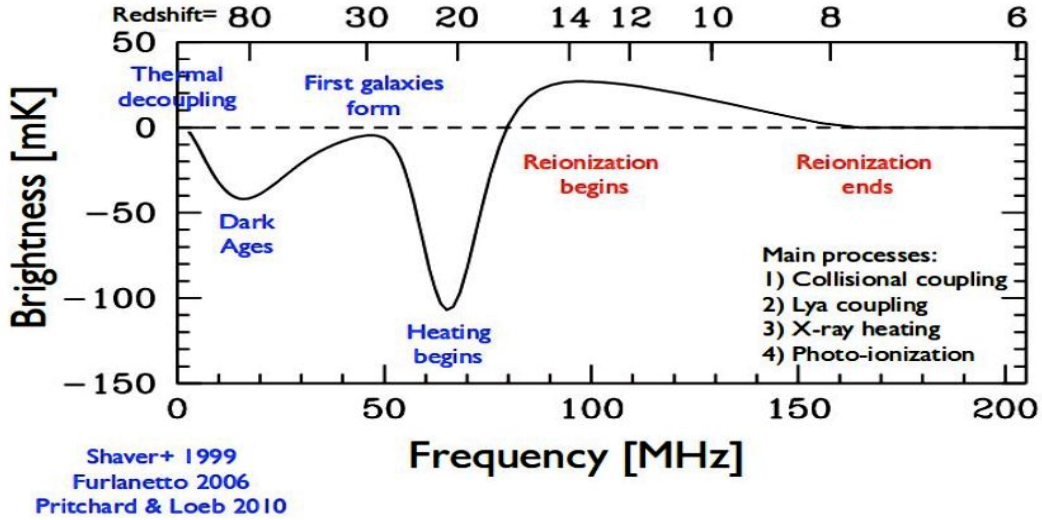

21CM Cosmology: Observational Challenges

- **Galactic and Extragalactic Foreground**

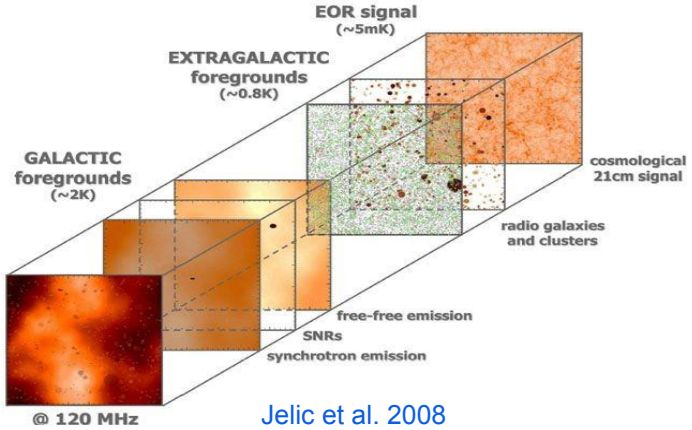

Jelic et al. 2008

- **Earth's Ionosphere**

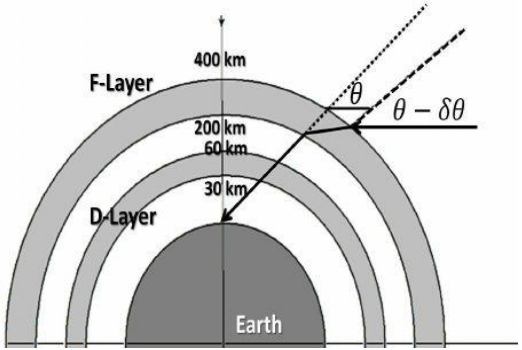

Fig : Schematic representation of the ionosphere showing the F- and D- layers (not scaled), which show the refraction. (Datta et al. 2016)

- **Radio Frequency Interference (RFI)**
- **Other Systematics effects**

- In the lower frequency the ionosphere affect the antenna beam which lead to chromatic mixing of spatial structure into spectral structure. (Vedantham et. al 2014, Datta et al. 2016).

- It can couple the relatively large angular fluctuations in the galactic foreground into spectral structures that may confuse global 21-cm signatures. (Mozdzen et al. (2016))

- It effects are significant especially with the Galactic Centre overhead.

- In E. Shen et al. 2022, it is demonstrated that, under turbulent ionospheric conditions, an error exceeding 5 percent in our understanding of the ionospheric parameters could result in false or null detection.

21CM GLOBAL SIGNAL: Effect of Ionosphere

Ionospheric Refraction due to F-layer

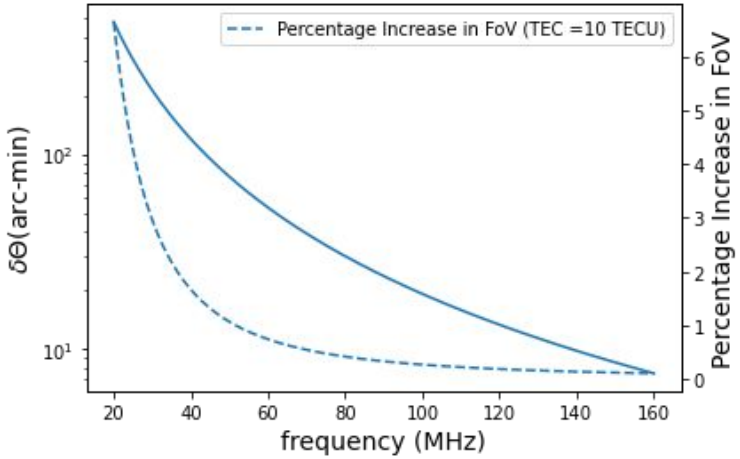

Increase in the effective FoV

$$T_{\rm sky}^{\rm iono}(\nu, t; \Theta_0, \Phi_0) = \int_0^{2\pi} d\Phi \times \int_0^{\pi/2} d\Theta B'(\nu, \Theta - \Theta_0 - \delta\theta(t), \Phi) \times T_{\rm sky}(\nu, \Theta - \Theta_0, \Phi - \Phi_0)\sin\Theta$$

Signal (T_{21}) + Foreground (T_{FG})

Ionospheric Absorption and Thermal Emission due to D-layer

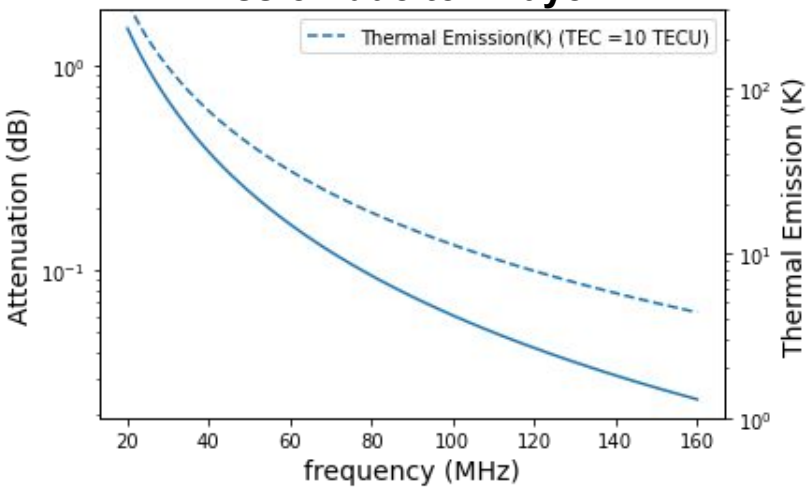

$$T_{Ant}^{iono}(\nu, TEC(t), \Theta_0, \Phi_0) = T_{sky}^{iono}(\nu, t; \Theta_0, \Phi_0) \times (1 - \tau(\nu, TEC(t)) + \tau(\nu, TEC(t)) * < T_e >$$

(Tripathi A. et al. 2024a, MNRAS)

Training Data Sets

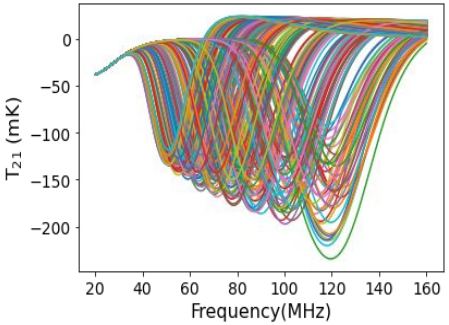

+

3rd order log(T)- log(v0) polynomial model

Foreground + Ionospheric effects

We use the Accelerated Reionization Era Simulations (ARES) code was designed to rapidly generate models for the global 21- cm signal. (Mirocha et al, 2012, 2015).

Training Parameters
21-cm Global Signal :- Jref, Jz0, Xz0, Tz0 Jdz, Xdz,Tdz
Foreground :- a0, a1, a2, a3 (Harker (2015))
Ionosphere :- TEC=10 TECU, Te= 800 K
Each Ionospheric parameters varies by ±1%.

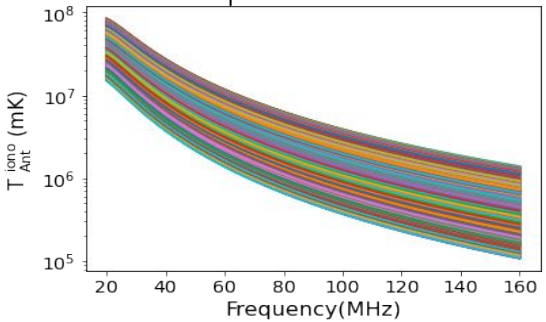

ANN Model

Saved ANN Model

Parameters	R2 Score	RMSE
J_{ref}	0.9614	0.0628
J_{z0}	0.9738	0.0605
X_{z0}	0.9713	0.0616
T_{z0}	0.9668	0.0577
J_{dz}	0.9634	0.0608
X_{dz}	0.9578	0.0658
T_{dz}	0.9595	0.0636
a_0	0.9810	0.0439
a_1	0.9655	0.0590
a_2	0.9586	0.0642
a_3	0.9610	0.0625
TEC	0.9658	0.0578
T_e	0.9728	0.0588

Test Data set
(Signal + Foreground +Ionospheric effect + Thermal Noise)

(Tripathi A. et al. 2024a, MNRAS)

Time Varying Ionosphere Model

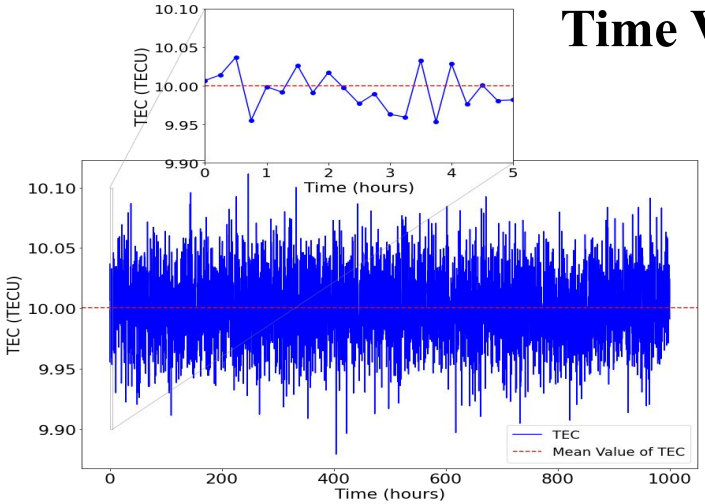

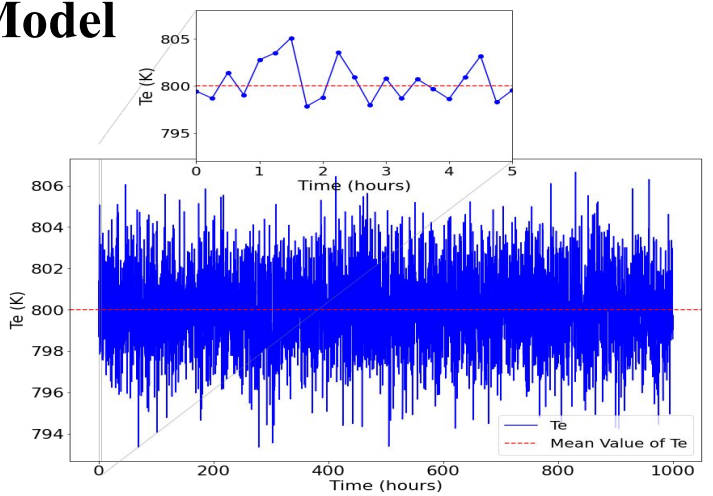

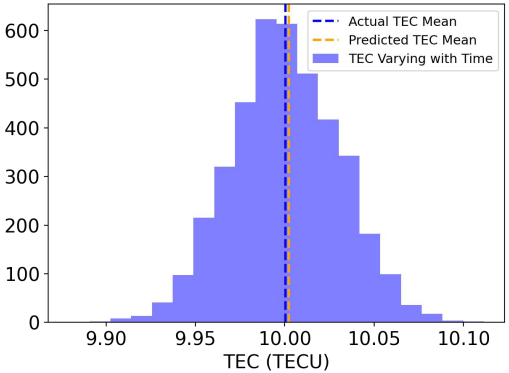

Tripathi A. et al. 2024a, MNRAS

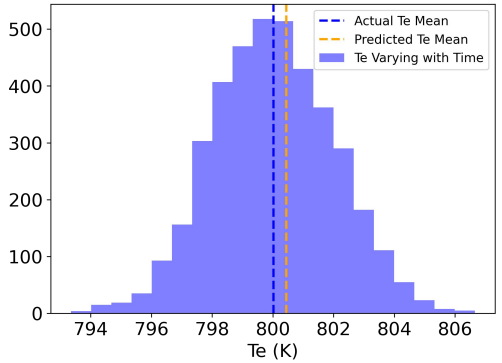

Time Varying Ionosphere Model

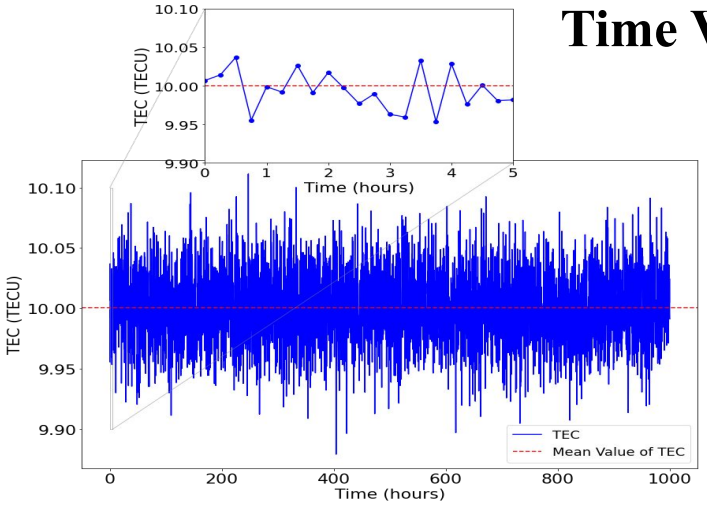

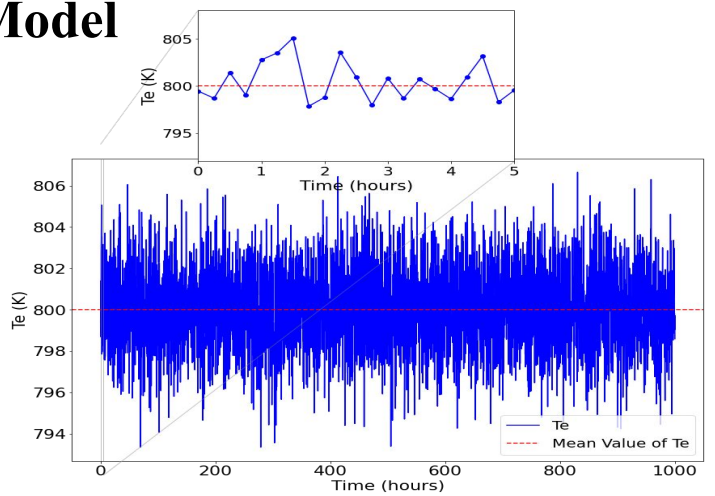

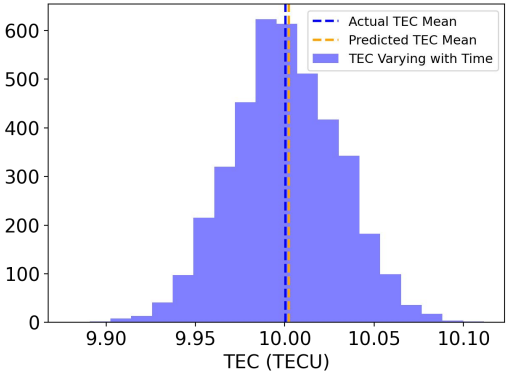

Tripathi A. et al. 2024a, MNRAS

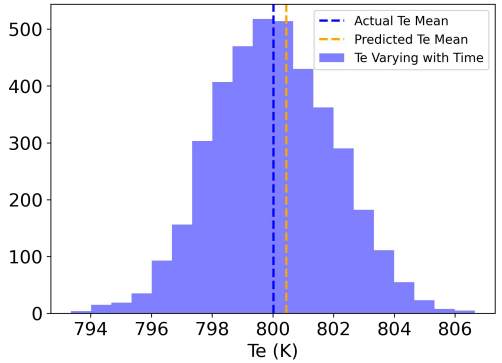

Conclusion: Simple ANN is robust in 21cm signal parameter estimates in presence of slowly varying ionosphere.

Motivation

- Without any observational constraints, the signal parameter space is enormously huge.

- Non-parametric techniques may produce biased inferences as they explore only a limited parameter space. To avoid bias, the data set includes multiple realizations of the signal generated by covering the whole parameter space.

- To reduce the computational burden of training Artificial Neural Networks (ANNs) and to achieve greater accuracy in extracting parameters from signals, it is necessary to employ sampling methods.

Charting Parameters Space using Sampling Technique

Random Sampling (Rand)

Samples assuming a uniform distribution. It may not be suitable for exploring high-dimensional spaces or regions of low probability.

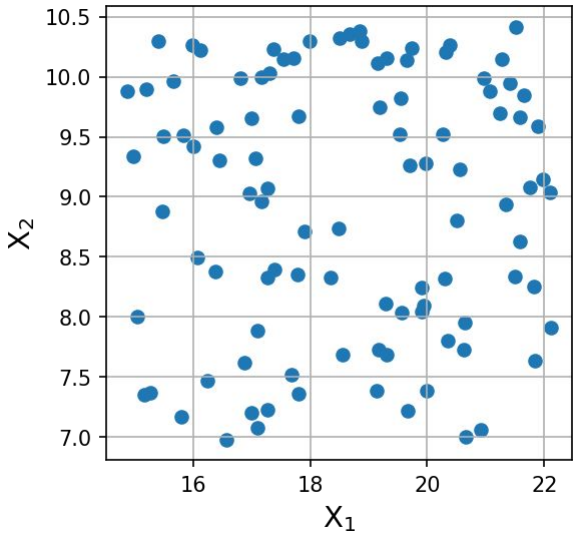

Latin Hypercube sampling (LHS)

Latin Hypercube a stratified sampling method. It divides the parameter space into equally sized bins and randomly selects samples within each bin.

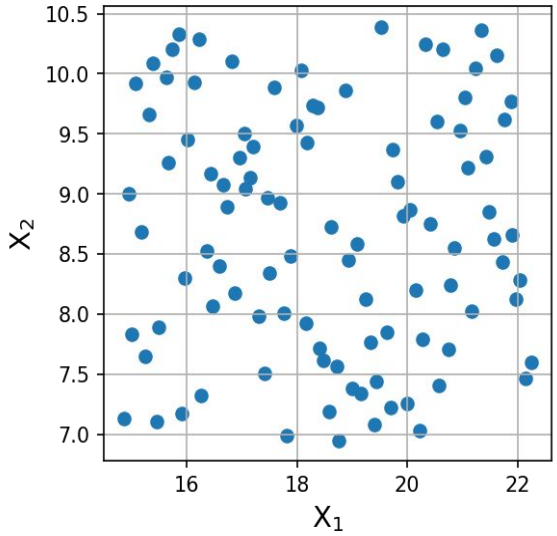

Hammersley sequence sampling (HSS)

Hammersley sampling is a quasi-random sampling technique used to generate low-discrepancy sequences of points in a hypercube.

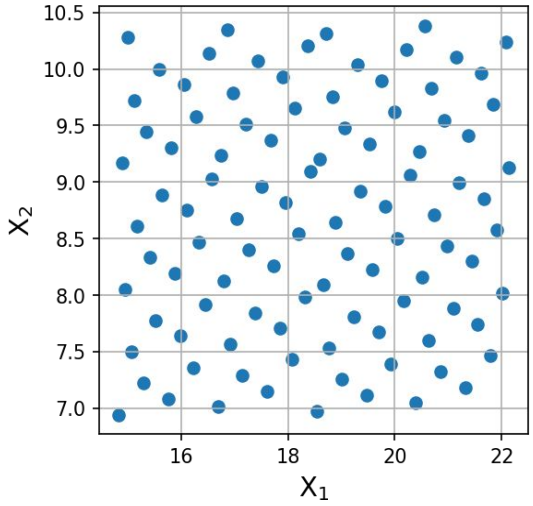

Training Dataset for Global Signal and Foreground

	Parametrized	
	Parameters	Ranges
Signal	J_{z0}	9.27, 27.81
	X_{z0}	4.34, 13.02
	T_{z0}	4.89, 14.65
	J_{dz}	1.65, 4.96
	T_{dz}	1.41, 4.23
	X_{dz}	1.42, 4.25
Foreground	a_0	2.97, 3.64
	a_1	-2.45, -2.37
	a_2	-0.082, -0.079
	a_3	0.027, 0.030

Harker et al. 2016b

Harker et al. 2015

Tab: The range of parameters used to build the training dataset.

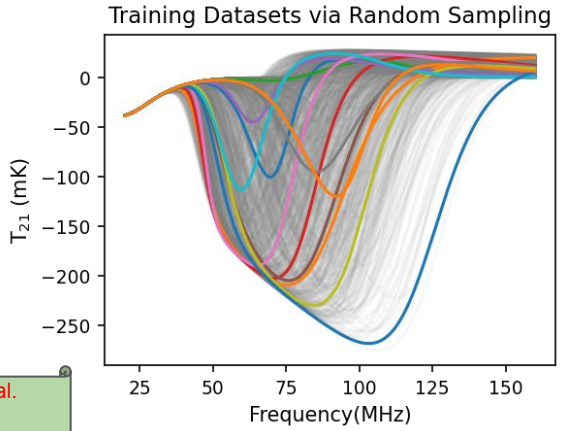

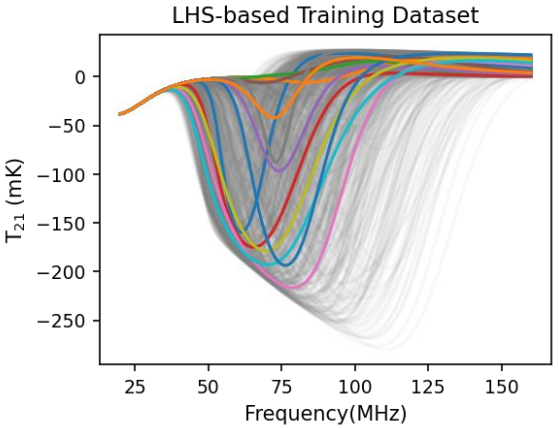

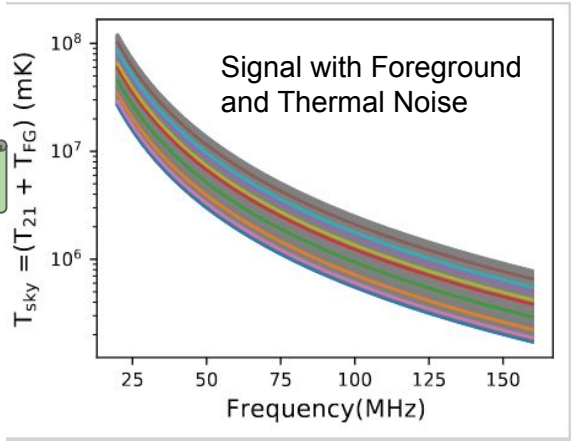

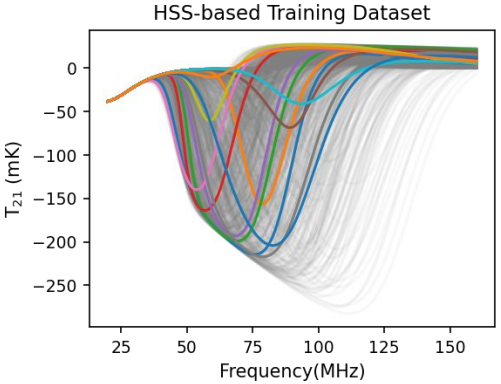

Tripathi A. et al. 2024b, JCAP, arXiv:2406.15832

ANN Model Prediction

Signal Only (R^2 Score)

Size		1000			5000			10000	
	HSS	LHS	Rand	HSS	LHS	Rand	HSS	LHS	Rand
Avg.	0.6744	0.6594	0.6379	0.9059	0.8937	0.8837	0.9259	0.9187	0.9210
J_{z0}	0.9471	0.9442	0.9389	0.9821	0.9780	0.9770	0.9868	0.9844	0.9859
X_{z0}	0.8797	0.8552	0.8687	0.9716	0.9681	0.9693	0.9751	0.9793	0.9758
T_{z0}	0.8589	0.8899	0.8908	0.9449	0.9431	0.9410	0.9686	0.9583	0.9615
J_{dz}	0.5514	0.4943	0.4107	0.9094	0.8790	0.8978	0.9323	0.9294	0.9258
X_{dz}	0.1942	0.1372	0.0807	0.7982	0.7759	0.7200	0.8395	0.8075	0.8161
T_{dz}	0.6151	0.6377	0.6377	0.8289	0.8180	0.7973	0.8450	0.8534	0.8607

Signal with Foreground and Thermal Noise (R^2 Score)

Size		10000			50000			200000	
	HSS	LHS	Rand	HSS	LHS	Rand	HSS	LHS	Rand
Total	0.7252	0.7534	0.7307	0.8673	0.8679	0.8738	0.9139	0.9296	0.9016
J_{z0}	0.8993	0.9020	0.9109	0.9573	0.9659	0.9626	0.9753	0.9798	0.9784
X_{z0}	0.8297	0.8962	0.8414	0.9447	0.9408	0.9447	0.9798	0.9796	0.9461
T_{z0}	0.8875	0.8689	0.8634	0.9315	0.9336	0.9396	0.9483	0.9554	0.9434
J_{dz}	0.2186	0.2677	0.2813	0.6651	0.7356	0.7244	0.8246	0.8603	0.8328
X_{dz}	0.6568	0.6968	0.6595	0.7838	0.7934	0.8025	0.8248	0.8458	0.8361
T_{dz}	0.4979	0.5837	0.5005	0.7953	0.7472	0.7875	0.8896	0.9083	0.7240
a_0	0.7229	0.7452	0.7292	0.8375	0.8672	0.8773	0.9086	0.9214	0.8889
a_1	0.9994	0.9997	0.9996	0.9989	0.9997	0.9999	0.9994	0.9999	0.9994
a_2	0.6095	0.6460	0.5964	0.8274	0.7659	0.7684	0.8606	0.9152	0.9363
a_3	0.9298	0.9281	0.9248	0.9319	0.9296	0.9311	0.9277	0.9302	0.9304

Signal Parameters Predicted by the ANN

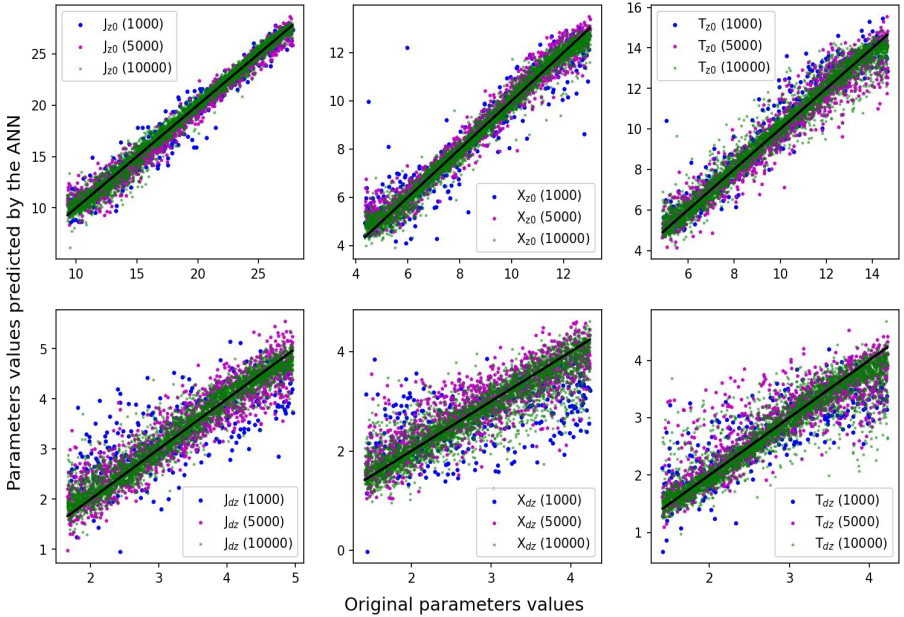

Tripathi A. et al. 2024b, JCAP, arXiv:2406.15832

ANN Model Prediction

Signal Only (R^2 Score)

Size		1000			5000			10000	
	HSS	LHS	Rand	HSS	LHS	Rand	HSS	LHS	Rand
Avg.	0.6744	0.6594	0.6379	0.9059	0.8937	0.8837	0.9259	0.9187	0.9210
J_{z0}	0.9471	0.9442	0.9389	0.9821	0.9780	0.9770	0.9868	0.9844	0.9859
X_{z0}	0.8797	0.8552	0.8687	0.9716	0.9681	0.9693	0.9751	0.9793	0.9758
T_{z0}	0.8589	0.8899	0.8908	0.9449	0.9431	0.9410	0.9686	0.9583	0.9615
J_{dz}	0.5514	0.4943	0.4107	0.9094	0.8790	0.8978	0.9323	0.9294	0.9258
X_{dz}	0.1942	0.1372	0.0807	0.7982	0.7759	0.7200	0.8395	0.8075	0.8161
T_{dz}	0.6151	0.6377	0.6377	0.8289	0.8180	0.7973	0.8450	0.8534	0.8607

Signal with Foreground and Thermal Noise (R^2 Score)

Size		10000			50000			200000	
	HSS	LHS	Rand	HSS	LHS	Rand	HSS	LHS	Rand
Total	0.7252	0.7534	0.7307	0.8673	0.8679	0.8738	0.9139	0.9296	0.9016
J_{z0}	0.8993	0.9020	0.9109	0.9573	0.9659	0.9626	0.9753	0.9798	0.9784
X_{z0}	0.8297	0.8962	0.8414	0.9447	0.9408	0.9447	0.9798	0.9796	0.9461
T_{z0}	0.8875	0.8689	0.8634	0.9315	0.9336	0.9396	0.9483	0.9554	0.9434
J_{dz}	0.2186	0.2677	0.2813	0.6651	0.7356	0.7244	0.8246	0.8603	0.8328
X_{dz}	0.6568	0.6968	0.6595	0.7838	0.7934	0.8025	0.8248	0.8458	0.8361
T_{dz}	0.4979	0.5837	0.5005	0.7953	0.7472	0.7875	0.8896	0.9083	0.7240
a_0	0.7229	0.7452	0.7292	0.8375	0.8672	0.8773	0.9086	0.9214	0.8889
a_1	0.9994	0.9997	0.9996	0.9989	0.9997	0.9999	0.9994	0.9999	0.9994
a_2	0.6095	0.6460	0.5964	0.8274	0.7659	0.7684	0.8606	0.9152	0.9363
a_3	0.9298	0.9281	0.9248	0.9319	0.9296	0.9311	0.9277	0.9302	0.9304

Signal Parameters Predicted by the ANN

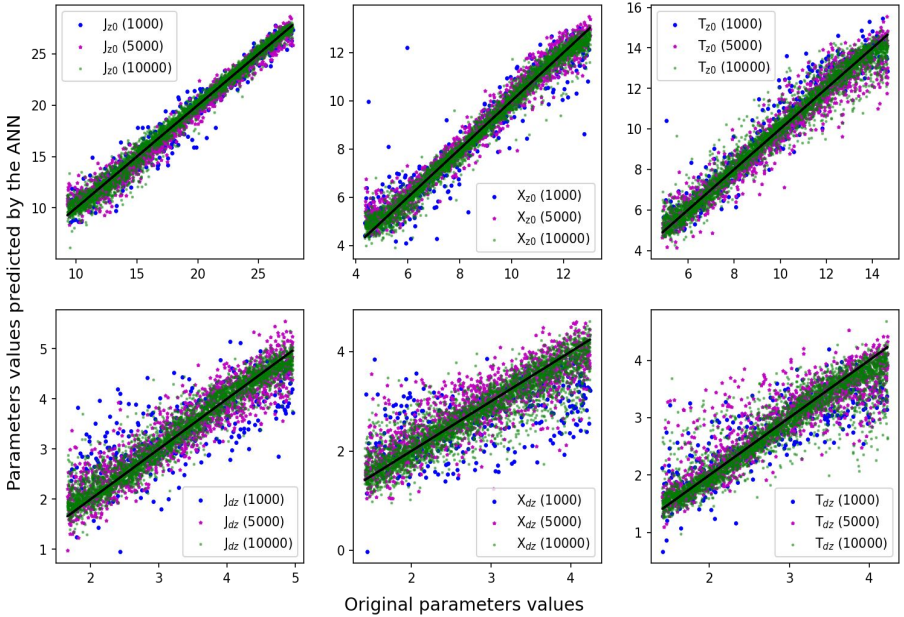

Tripathi A. et al. 2024b, JCAP, arXiv:2406.15832

ANN Model Prediction

Signal Only (R^2 Score)

Size		1000			5000			10000	
	HSS	LHS	Rand	HSS	LHS	Rand	HSS	LHS	Rand
Avg.	0.6744	0.6594	0.6379	0.9059	0.8937	0.8837	0.9259	0.9187	0.9210
J_{z0}	0.9471	0.9442	0.9389	0.9821	0.9780	0.9770	0.9868	0.9844	0.9859
X_{z0}	0.8797	0.8552	0.8687	0.9716	0.9681	0.9693	0.9751	0.9793	0.9758
T_{z0}	0.8589	0.8899	0.8908	0.9449	0.9431	0.9410	0.9686	0.9583	0.9615
J_{dz}	0.5514	0.4943	0.4107	0.9094	0.8790	0.8978	0.9323	0.9294	0.9258
X_{dz}	0.1942	0.1372	0.0807	0.7982	0.7759	0.7200	0.8395	0.8075	0.8161
T_{dz}	0.6151	0.6377	0.6377	0.8289	0.8180	0.7973	0.8450	0.8534	0.8607

Signal with Foreground and Thermal Noise (R^2 Score)

Size		10000			50000			200000	
	HSS	LHS	Rand	HSS	LHS	Rand	HSS	LHS	Rand
Total	0.7252	0.7534	0.7307	0.8673	0.8679	0.8738	0.9139	0.9296	0.9016
J_{z0}	0.8993	0.9020	0.9109	0.9573	0.9659	0.9626	0.9753	0.9798	0.9784
X_{z0}	0.8297	0.8962	0.8414	0.9447	0.9408	0.9447	0.9798	0.9796	0.9461
T_{z0}	0.8875	0.8689	0.8634	0.9315	0.9336	0.9396	0.9483	0.9554	0.9434
J_{dz}	0.2186	0.2677	0.2813	0.6651	0.7356	0.7244	0.8246	0.8603	0.8328
X_{dz}	0.6568	0.6968	0.6595	0.7838	0.7934	0.8025	0.8248	0.8458	0.8361
T_{dz}	0.4979	0.5837	0.5005	0.7953	0.7472	0.7875	0.8896	0.9083	0.7240
a_0	0.7229	0.7452	0.7292	0.8375	0.8672	0.8773	0.9086	0.9214	0.8889
a_1	0.9994	0.9997	0.9996	0.9989	0.9997	0.9999	0.9994	0.9999	0.9994
a_2	0.6095	0.6460	0.5964	0.8274	0.7659	0.7684	0.8606	0.9152	0.9363
a_3	0.9298	0.9281	0.9248	0.9319	0.9296	0.9311	0.9277	0.9302	0.9304

Tripathi A. et al. 2024b, JCAP, arXiv:2406.15832

Signal Parameters Predicted by the ANN

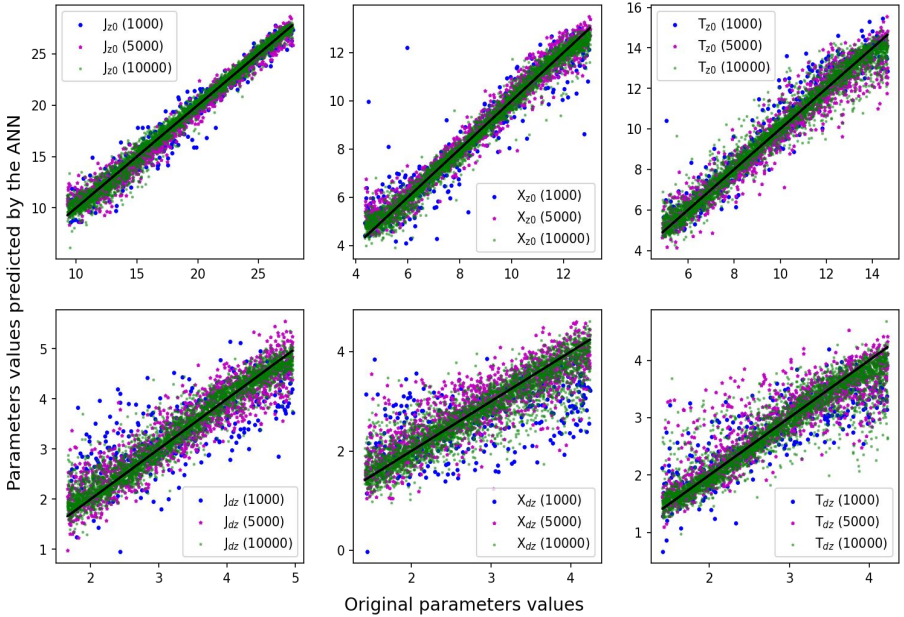

1) In the lower sample size Hammersley perform slightly better in the lower dimensions.

2) At large number of sample size all sampling methods conserved at the same point.

Generalizability Test of the ANN Models

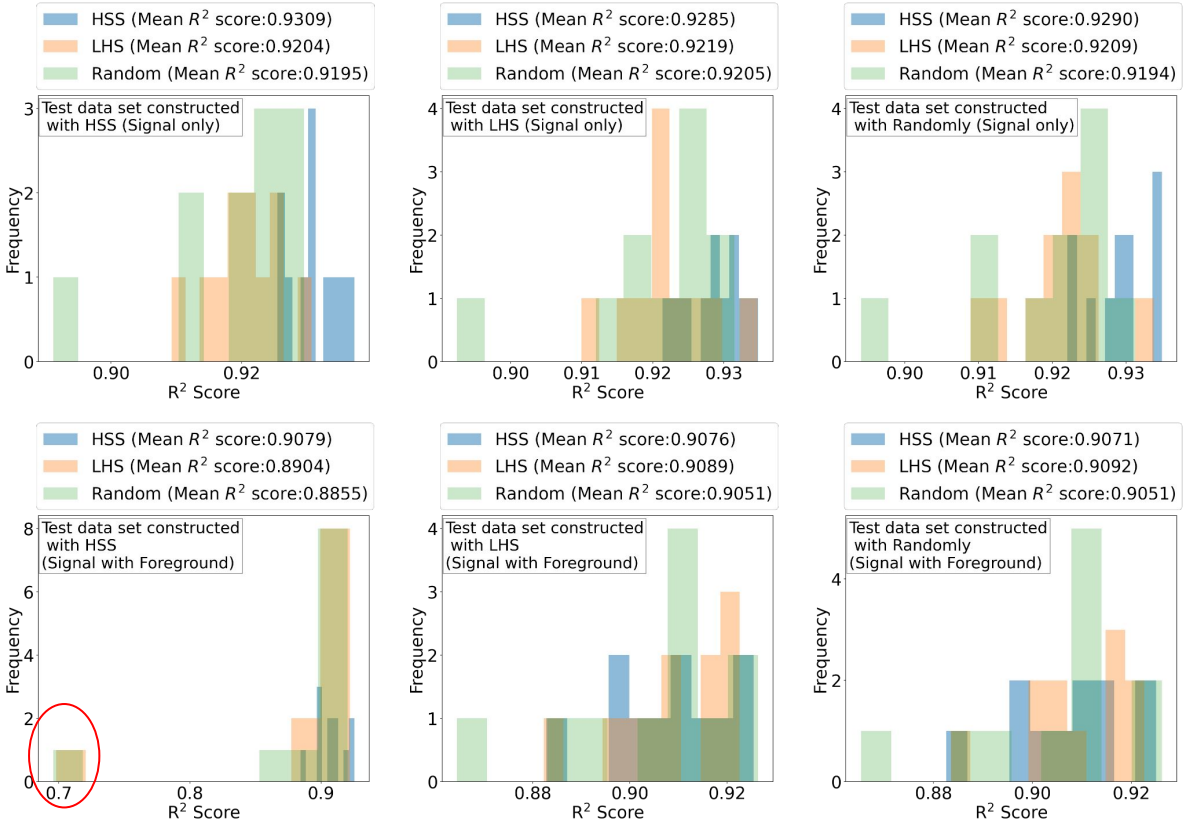

Fig : This shows the ANN model predictions for various trials trained on datasets sampled using HSS, LHS, and Random Sampling methods with optimal sample sizes. Histograms depict ANN prediction accuracy measured in terms of R^2 scores.

Generalizability Test of the ANN Models

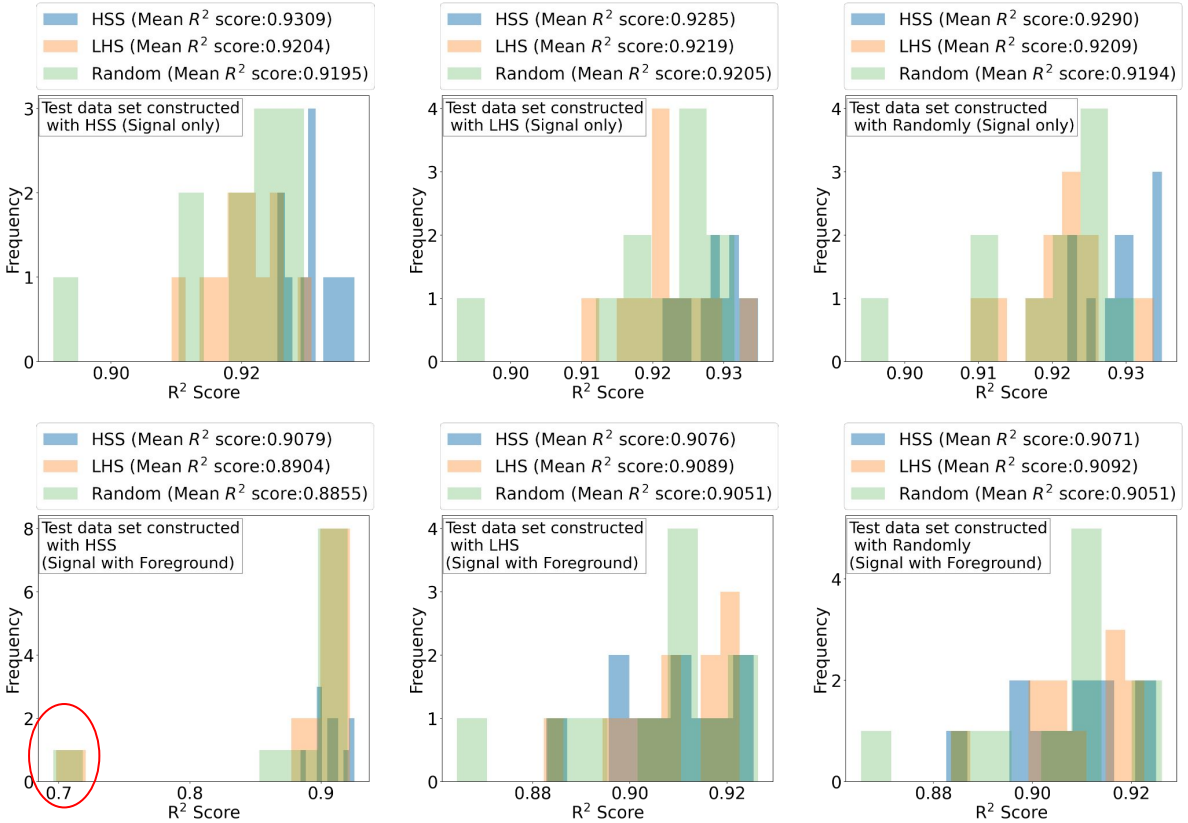

Fig : This shows the ANN model predictions for various trials trained on datasets sampled using HSS, LHS, and Random Sampling methods with optimal sample sizes. Histograms depict ANN prediction accuracy measured in terms of R^2 scores.

Takeaway & Summary

- Achieving a high level of accuracy in training the ANN model necessitates an ample number of samples, regardless of the sampling technique employed.
- The number of drawing of the samples highly dependent on the dimensionality and complexity.
- Among the given sampling techniques we found the model train with Hammersley Sequence are more robust.

Tripathi A. et al. 2024b, Published in JCAP, arXiv:2406.15832

ANN Model Prediction with different Signal Model

Signal Only (R^2 Score)

Size		1000			5000			10000	
	HSS	LHS	Rand	HSS	LHS	Rand	HSS	LHS	Rand
Avg.	0.9155	0.9252	0.9214	0.9392	0.9367	0.9346	0.9447	0.9446	0.9418
$f_{*}.f_{esc}$	0.9936	0.9922	0.9893	0.9945	0.9957	0.9940	0.9974	0.9970	0.9944
$f_{X,h}.f_{X}$	0.8255	0.8373	0.8408	0.8785	0.8682	0.8642	0.8837	0.8737	0.8783
N_{α}	0.9275	0.9454	0.9341	0.9531	0.9539	0.9555	0.9531	0.9532	0.9527

Signal with Foreground and Thermal Noise (R^2 Score)

Size		10000			50000			100000	
	HSS	LHS	Rand	HSS	LHS	Rand	HSS	LHS	Rand
Avg.	0.9277	0.9187	0.9018	0.9505	0.9448	0.9429	0.9670	0.9647	0.9608
$f_{*}.f_{esc}$	0.9813	0.9532	0.9776	0.9890	0.9510	0.9634	0.9843	0.9903	0.9860
$f_{X,h}.f_{X}$	0.8574	0.8727	0.8272	0.8807	0.8502	0.8570	0.9139	0.9168	0.9142
N_{α}	0.9395	0.9398	0.8502	0.9512	0.9454	0.9405	0.9620	0.9563	0.9629
a_0	0.9925	0.9978	0.9960	0.9968	0.9959	0.9969	0.9988	0.9986	0.9973
a_1	0.9996	0.9969	0.9974	0.9993	0.9982	0.9998	0.9999	0.9991	0.9998
a_2	0.7921	0.7281	0.7291	0.9080	0.9386	0.9084	0.9590	0.9415	0.9242
a_3	0.9317	0.9427	0.9353	0.9340	0.9327	0.9337	0.9505	0.9504	0.9400

Signal Parameters Predicted by the ANN

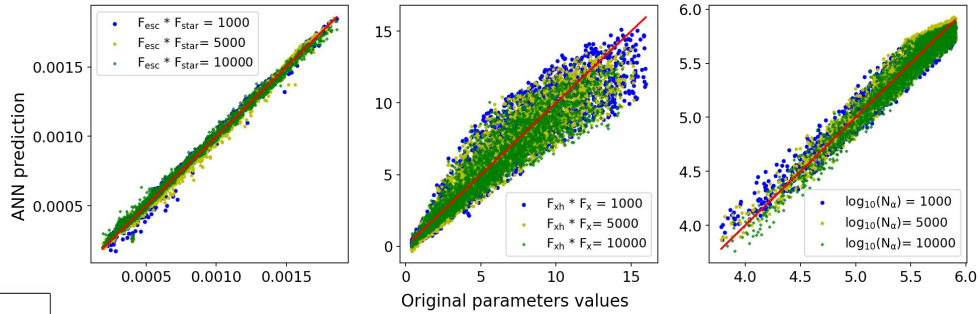

- Consistent trends in prediction accuracy were observed across different Signal Models.

Tripathi A. et al. 2024b, Published in JCAP, arXiv:2406.15832

Dynamic Ionospheric Effects

Ionospheric effect on Antenna Beam

$$\hat{B}(\nu, \theta, \phi) = B(\nu, \theta - \delta\theta, \phi) \cdot L(\nu, \theta - \delta\theta, \phi)$$

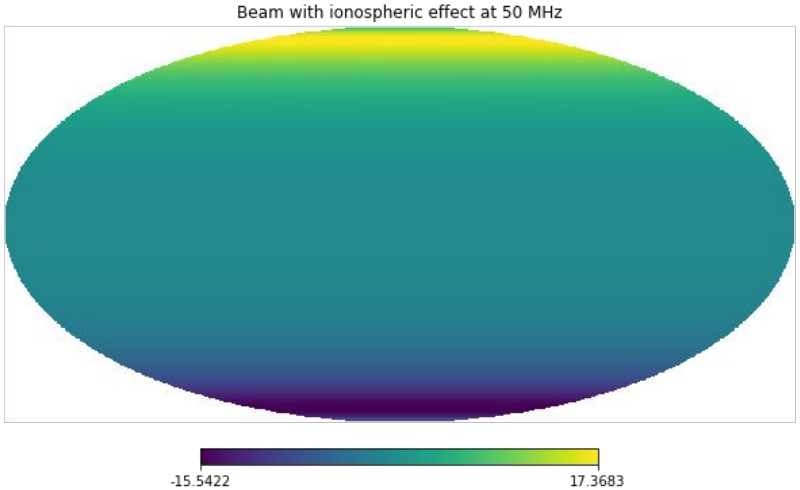

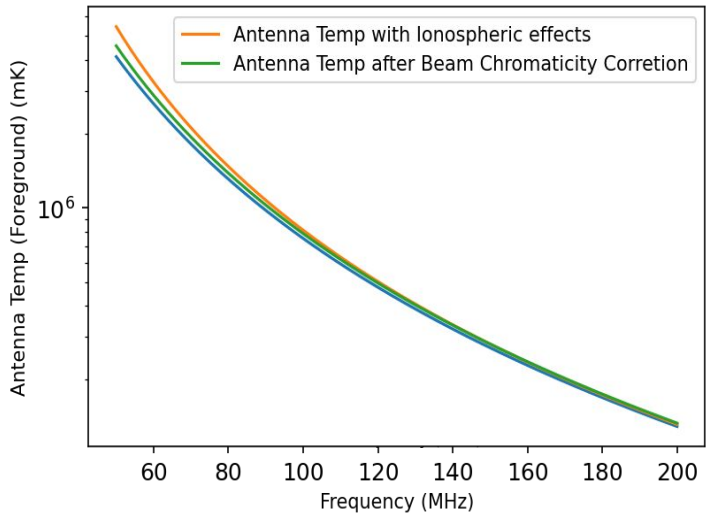

$$B_{\text{factor}}(\nu) = \frac{\int_\Omega T_{\text{sky}}(\nu_{150}, \Omega) B(\nu, \Omega) \mathrm{d}\Omega}{\int_\Omega T_{\text{sky}}(\nu_{150}, \Omega) B(\nu_{150}, \Omega) \mathrm{d}\Omega},$$

$$T_{\text{A}}(\nu) = \int_0^{2\pi} d\phi \int_0^{\pi/2} B(\nu, \theta, \phi) \left[T_{\text{te}}(\nu, \theta) + \mathcal{L}(\nu, \theta) \times \widehat{T}_{\text{sky}}(\nu, \theta, \phi) \right] \sin\theta d\theta.$$

Vedantham et. al 2014, Datta et al. 2016, Mozdzen et al. (2016), E. Shen et al. (2021), Tripathi A. et al. 2024, Wang et al. 2024

2 Steps ANNs Training

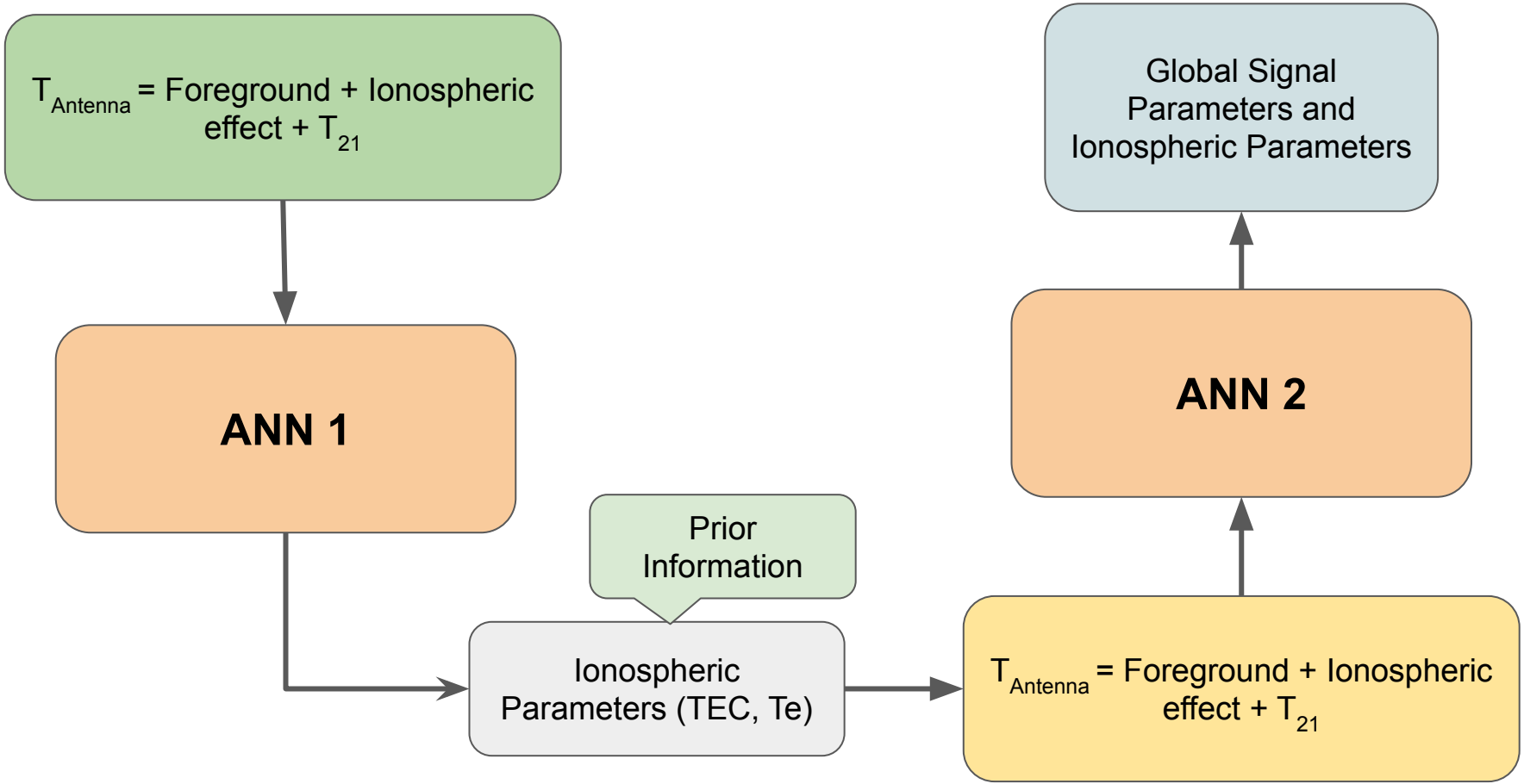

ANN prediction of Ionospheric Parameters (ANN1)

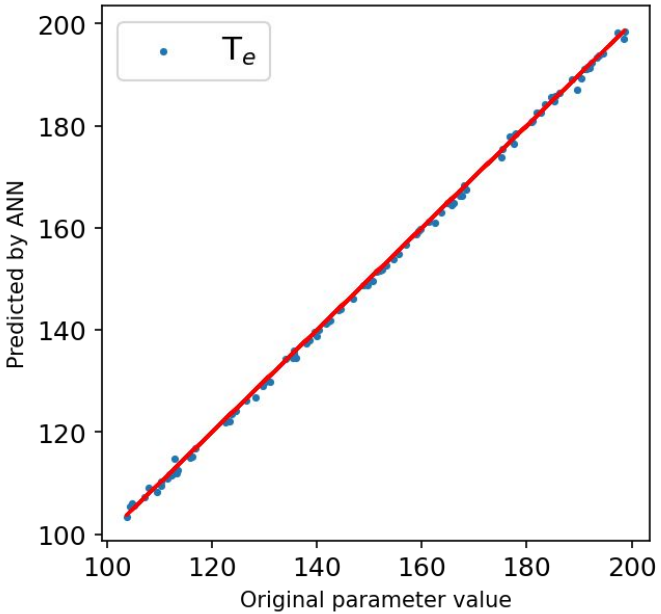

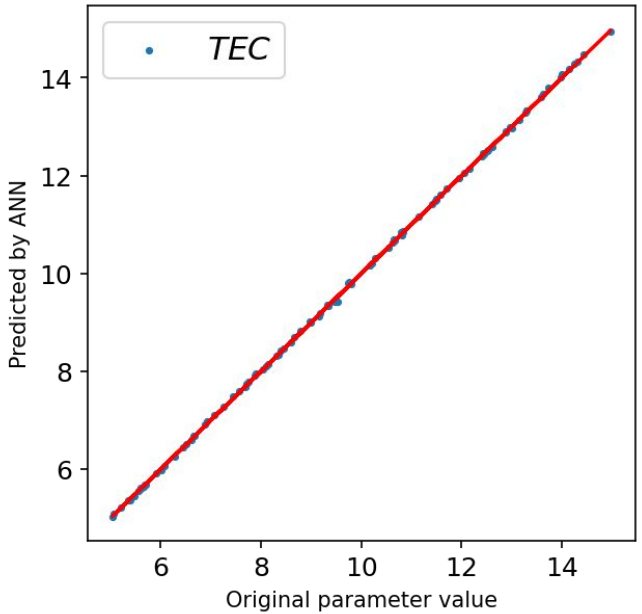

R^2 score ≃ 0.99

Tripathi A. et al. in prep.

ANN 2 prediction

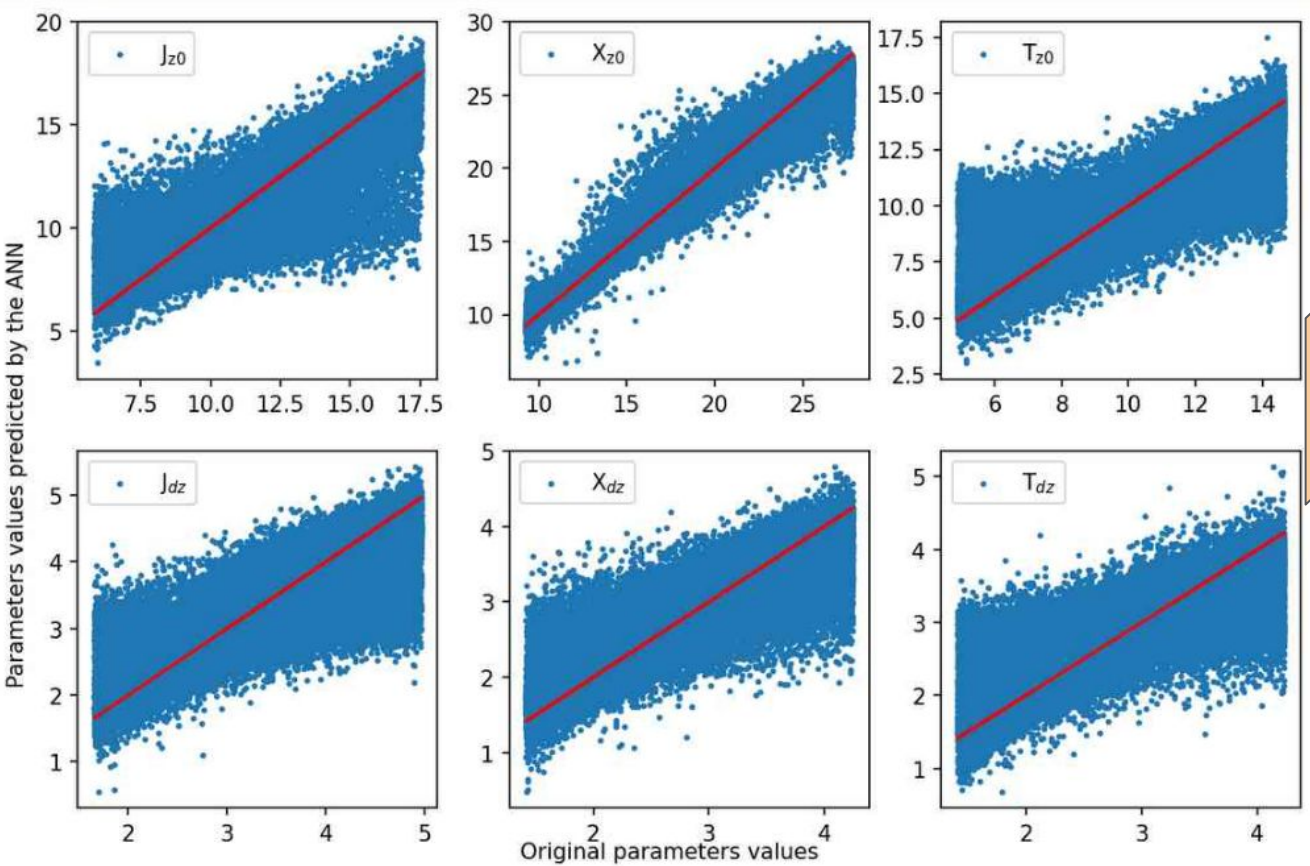

R^2 score ranging 0.60 to 0.90

Tripathi A. et al. in prep.

ANN 2 prediction

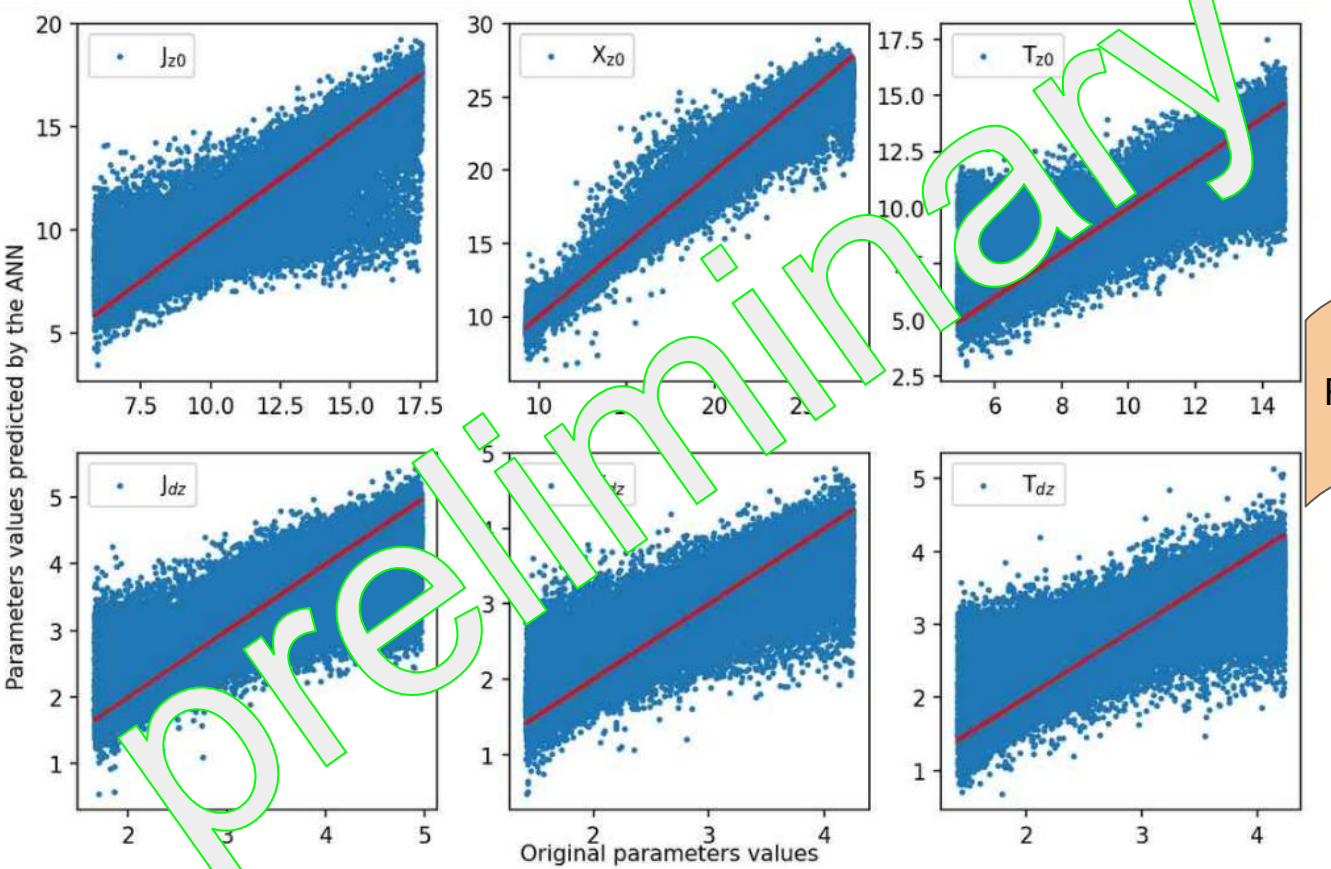

R^2 score ranging 0.60 to 0.90

Tripathi A. et al. in prep.

Time Varying Global Sky Model with Ionospheric effects

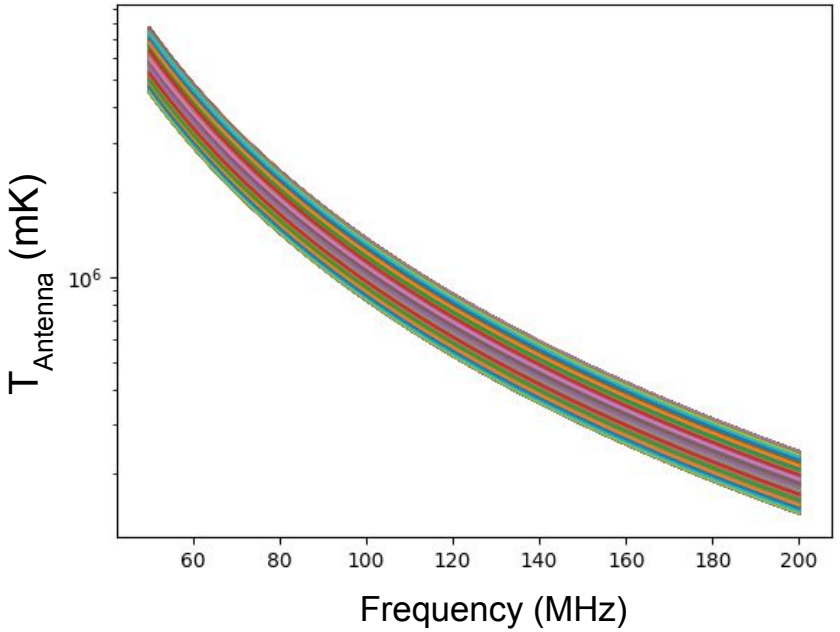

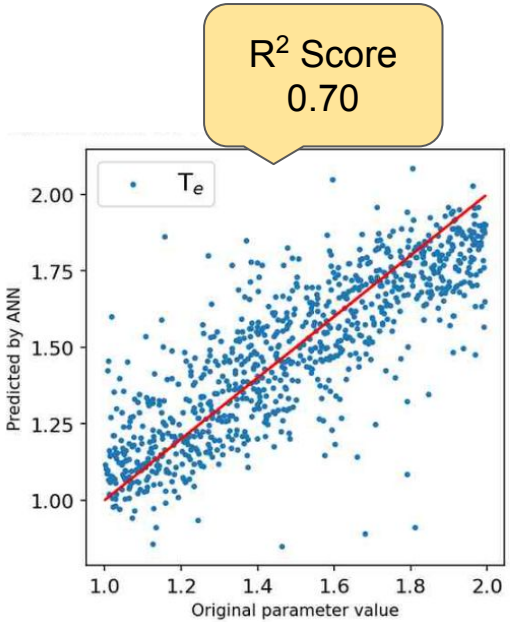

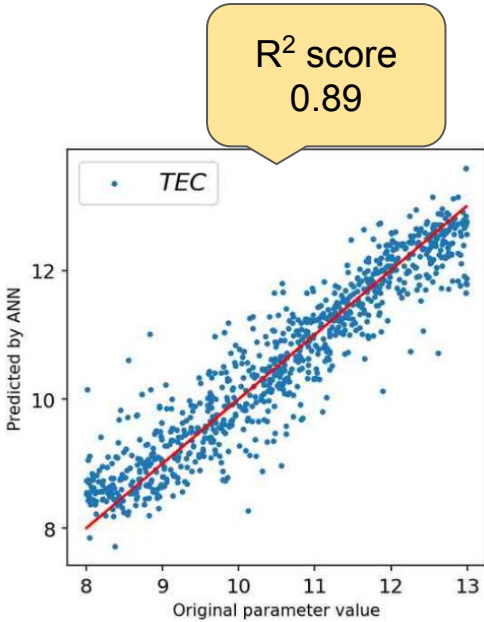

Tripathi A. et al. in prep.

Ongoing Work

- Further plan to study effects of Chromatic Effects of Soil and Grounding.

- Plan to compare these effects across various antenna beams to enhance our pipeline's robustness.

Thank You.

I am seeking a Postdoctoral position. If anyone is hiring, please let me know!

Email : anshumantripathi85@gmail.com

21 cm line

Arises due to "spin-flip" transition in hydrogen atom.

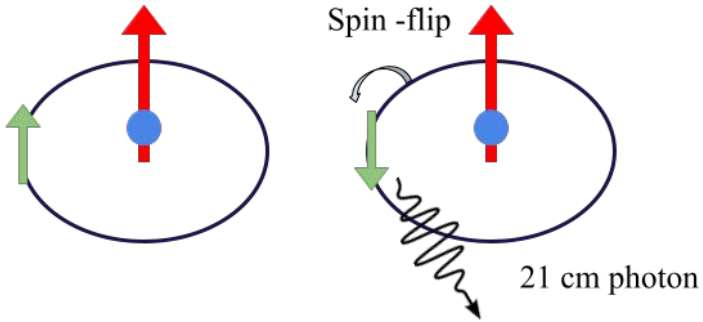

Triplet state Higher energy	Singlet state Lower energy

Spin Temp

- Intrinsically forbidden
- Einstein' A coefficient:
  Probability of transition:
  $A_{10} = 2.85 \times 10^{-15}$s
- Lifetime: 10^7 years!

- Abundance of Hydrogen(75%)
- Coupling:
  Collisions
  Lyman α pumping
  Scattering with Cosmic microwave background(CMB)

Make it happen and seen!

✘ Ratio of number of H atoms in triplet to singlet state..

$$\left(\frac{n_1}{n_0}\right) = 3\exp\left(\frac{-T_*}{T_s}\right)$$

The First Dawn

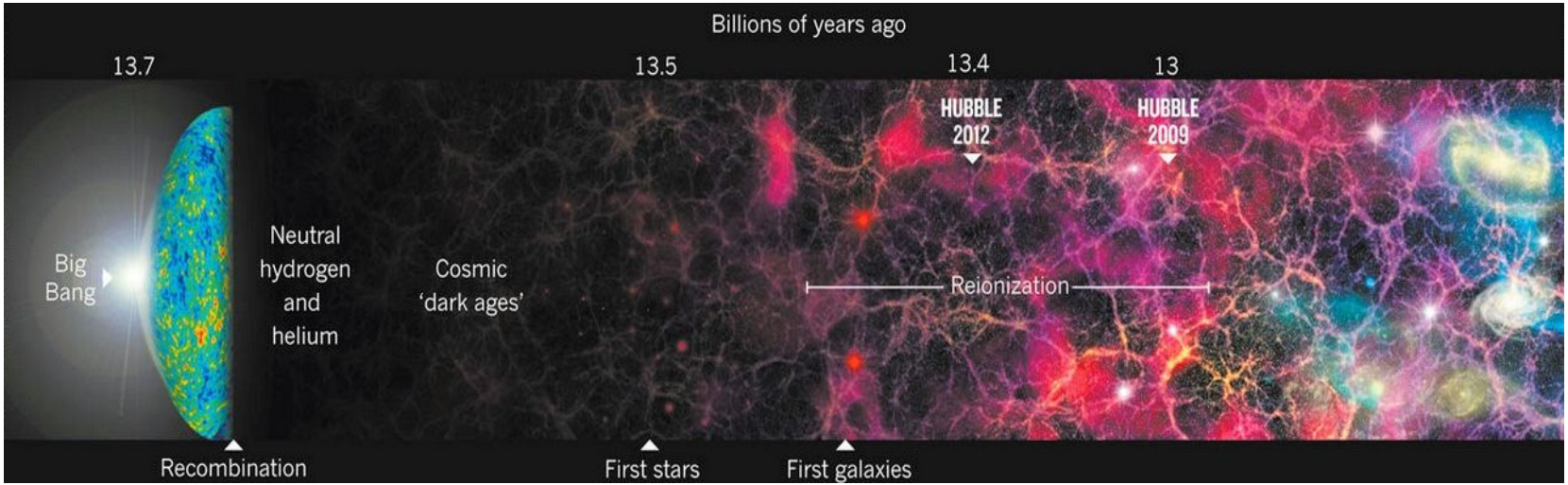

Source:https://astrobites.org/wp-content/uploads/2015/05/cover.png